CMLS, Cell. Mol. Life Sci. 62 (2005) 386–395
1420-682X/05/030386-10
DOI 10.1007/s00018-004-4446-8

CMLS Cellular and Molecular Life Sciences

Research Article

Confocal microscopy and biochemical analysis reveal spatial and functional separation between anandamide uptake and hydrolysis in human keratinocytes

S. Oddi[a], M. Bari[a], N. Battista[a], D. Barsacchi[a], I. Cozzani[a] and M. Maccarrone[a,b,*]

[a] Department of Biomedical Sciences, University of Teramo, Piazza A. Moro 45, 64100 Teramo (Italy), Fax: + 39 0861 412583, e-mail: mmaccarrone@unite.it
[b] IRCCS C. Mondino, Mondino-Tor Vergata-Santa Lucia Center for Experimental Neurobiology, Via Ardeatina 306, 00179 Rome (Italy)

Received 11 October 2004; received after revision 24 November 2004; accepted 7 December 2004

Abstract. The signaling activity of anandamide (AEA) is terminated by its uptake across the cellular membrane and subsequent intracellular hydrolysis by the fatty acid amide hydrolase (FAAH). To date, the existence of an AEA membrane transporter (AMT) independent of FAAH activity remains questionable, although it has been recently corroborated by pharmacological and genetic data. We performed confocal microscopy and biochemical analysis in human HaCaT keratinocytes, in order to study the cellular distribution of AMT and FAAH. We found that FAAH is intracellularly localized as a punctate staining partially overlapping with the endoplasmic reticulum. Consistently, subcellular fractionation and reconstitution of vesicles from membranes of different compartments demonstrated that FAAH activity was localized mainly in microsomal fractions, whereas AMT activity was almost exclusively in plasma membranes. These results provide the first morphological and biochemical evidence to support the view that transport and hydrolysis are two spatially and functionally distinct processes in AEA degradation.

Key words. Differentiation; endocannabinoid; fatty acid amide hydrolase; HaCaT cell; lipid raft; membrane transport.

Amides, esters, and ethers of long-chain polyunsaturated fatty acids, collectively referred to as 'endocannabinoids', represent a growing family of lipid signaling mediators found in several tissues with diverse biological effects [1–4]. The main members of this group of molecules are anandamide (N-arachidonoylethanolamine, AEA) and 2-arachidonoylglycerol (2-AG) [5, 6]. These two lipids act as endogenous cannabinoids by binding to and functionally activating both type-1 (CB1R) and type-2 (CB2R) cannabinoid receptors present in nervous and peripheral cells [7, 8], thus mimicking some effects of Δ^9-tetrahydrocannabinol, the psychoactive principle of *Cannabis sativa* extracts [9].

The signaling action of AEA via CB1R and CB2R depends on its extracellular concentration, and is terminated by cellular uptake and intracellular degradation by fatty acid amide hydrolase (FAAH) [10, 11]. The latter enzyme has been crystallized [12] and the details of its catalytic mechanism have been disclosed [13]. On the other hand, there is still considerable debate on the mechanism of AEA uptake and on the identity of a purported AEA membrane transporter (AMT) [see ref. 14 for a recent review]. In fact, two alternative models have been proposed to explain AEA transport through cell membranes: the first suggests a process of facilitated diffusion mediated

* Corresponding author.

by AMT; the second postulates that AEA uptake is a simple diffusion driven by AEA hydrolysis via FAAH [14–17]. Although FAAH activity might variably contribute to AEA uptake [18, 19], recent studies, performed with specific inhibitors of AEA internalization and with animals genetically devoid of FAAH, have strengthened the evidence for a true plasma membrane-associated AEA carrier independent of FAAH [18, 20, 21]. Nonetheless, direct evidence to support this view in cells with a normal genetic background for FAAH is still missing.

Here, we sought to address the contribution of FAAH to AEA uptake via AMT by separating for the first time these processes in cultured human keratinocytes. To this end, we performed the first confocal microscopy characterization of FAAH in the human HaCaT cell line, where we have recently described a fully functional 'endocannabinoid system' [22]. As already proposed for other cell types based on immunocytochemical evidence [23–25], confocal microscopy showed that FAAH is localized intracellularly as a vesicular-like staining, has no association with the plasma membranes, and is partially co-localized with the endoplasmic reticulum. These morphological data were corroborated by measuring FAAH activity in subcellular fractions, showing that AEA hydrolase was primarily confined to the endomembrane compartment. Moreover, by means of reconstituted vesicles derived from purified membrane fractions, we were able to demonstrate that AMT activity is retained by plasma membrane vesicles devoid of FAAH, thereby indicating that AEA hydrolase activity is not necessary for AEA membrane transport.

Taken together, our findings provide direct morphological and biochemical evidence for a spatial and functional separation of the two steps of AEA signaling inactivation.

Materials and methods

Materials

Chemicals were of the purest analytical grade. N-(2-methyl-4-hydroxy-phenyl)-arachidonamide (VDM11) was from Tocris-Cookson (Bristol, UK), methyl-arachidonoyl fluorophosphonate (MAFP) and cyclohexylcarbamic acid 3′-carbamoyl-biphenyl-3-yl ester (URB597) were from Cayman Chemicals (Ann Arbor, Mich.). [^{3}H]AEA (223 Ci/mmol) was from NEN DuPont de Nemours (Cologne, Germany). Fluorescein diacetate was from Sigma (St. Louis, Mo.). Rabbit anti-caveolin-1 (CAV-1) polyclonal antibodies were from Santa Cruz Biotechnologies (Santa Cruz, Calif.), and goat anti-rabbit alkaline phosphatase conjugates were from Bio-Rad (Hercules, Calif.). (*S*)-1′-(4-hydroxybenzyl)-oleoylethanolamide (OMDM-1) was a kind gift of Dr. S. Marinelli (Experimental Neurology, IRCCS Fondazione Santa Lucia, Rome, Italy), and N-piperidino-5-(4-chlorophenyl)-1-(2,4-dichlorophenyl)-4-methyl-3-pyrazole carboxamide (SR141716) was a kind gift of Sanofi-Synthelabo Recherche (Montpellier, France).

Cell culture and treatment

HaCaT cells, kindly provided by Prof. N. E. Fusenig (German Cancer Research Center, Heidelberg, Germany), were cultured in a mixture of D-MEM and F12 media (1:1, v/v) supplemented with 10% fetal calf serum, 0.05 mM $CaCl_2$ and 100 units/ml streptomycin/penicillin at 37 °C in a 5% CO_2 humidified atmosphere. Cell differentiation was induced by treating cells with 12-O-tetradecanoylphorbol 13-acetate (TPA, 10 ng/ml) and $CaCl_2$ (1.2 mM; referred to henceforth as Ca in the rest of the paper) for 6 h, 24 h or 5 days. Control cells were collected before confluence.

Confocal microscopy

For confocal microscopy, HaCaT cells were grown on collagen-coated glass coverslips and either left untreated or incubated with TPA/Ca for the indicated periods. Cells were fixed with 4% paraformaldehyde for 10 min at room temperature (RT), and then permeabilized with 0.1% Triton X-100 in phosphate-buffered saline (PBS) for 2 min at 4 °C. After a blocking step in 5% bovine serum albumin (BSA) in PBS for 30 min at RT, cells were incubated for 1 h at RT with primary antibodies diluted as needed in blocking solution. In this study, we used the following antibodies: anti-FAAH polyclonal antibodies (1:100; Primm, Milan, Italy) [22]; mouse monoclonal anti-K1 (1:1000; Abcam, Cambridge, UK), mouse monoclonal anti-calnexin (1:500) and mouse monoclonal anti-alpha adaptin1 (1:100) antibodies from ABR (Golden, Colo.). Mitochondria and lysosomes were stained using, respectively, MitoTracker Red CMX Ros and LysoTracker Red DND-99 according to the manufacturer's instructions (Molecular Probes, Eugene, Ore.). Secondary antibodies (anti-mouse and anti-rabbit Alexa Fluor 488 or Alexa Fluor 568 conjugated immunoglobulins from Molecular Probes) were diluted 1:500 in blocking solution and incubated with the samples for 30 min at RT. After washing, the coverslips were mounted using a Prolong antifade kit (Molecular Probes) and visualized by Eclipse TE200 confocal microscopy (Nikon Instruments, Tokyo, Japan).

Membrane fractionation

To obtain membrane preparations enriched in plasma membranes and microsomes, HaCaT cells were fractionated as described elsewhere [26]. Briefly, HaCaT cells, grown on twenty 15-cm Corning dishes, were detached from plates and washed three times with PBS prior to lysis in 1 ml of LB buffer [250 mM sucrose, 20 mM Tricine pH 7.8, 1 mM EDTA, 1 mM 4-(2-aminoethyl)benzenesulfonyl fluoride (AEBSF), 1 mM dithiothreitol (DTT)] in a loose-fitting dounce homogenizer. The homogenate

was centrifuged at 1400 g for 10 min at 4 °C. The postnuclear supernatant, representing the crude membrane preparation, was layered on top of 23 ml of 30% Percoll in LB buffer, and centrifuged at 84,000 g for 30 min in a Beckman Ti 60 rotor (Fullerton, Calif.). After centrifugation, plasma membranes were collected as a white visible band at ~ 6 cm from the bottom of the centrifuge tube. Alternatively, postnuclear supernatant obtained as above was fractionated through a sequence of differential centrifugation steps to obtain a postmitochondrial (10,000 g for 10 min) supernatant and a mitochondrial pellet. Microsomes were pelleted by centrifugation of the postmitochondrial supernatant at 100,000 g for 2.5 h.

Enzyme assays

Membrane fractions were characterized for the presence of plasma membrane and rough endoplasmic reticulum enzyme markers: alkaline phosphatase and NADPH cytochrome c reductase, respectively. Alkaline phosphatase was measured by the method of Engstrom [27], and NADPH cytochrome c reductase was assayed according to Williams and Kamin [28]. The activity of FAAH was determined in homogenates of whole HaCaT cells, crude membrane (CM), plasma membrane (PM) or microsomial membrane (MM) fractions (20 µg/test), by measuring the release of [^{3}H]arachidonic acid from 10 µM [^{3}H]AEA at pH 9.0, using reversed-phase-high-performance liquid chromatography [22]. The effect of 100 nM MAFP [29] or 10 nM URB597 [30], selective FAAH inhibitors, or of 5 µM OMDM-1, a selective AMT inhibitor [31], or of 100 nM SR141716, a selective antagonist of CB1 receptors [18], on the hydrolysis of 10 µM [^{3}H]AEA was determined by adding each substance directly to the incubation medium. Protein concentration in all samples was determined by the Bradford assay, following the manufacturer's instructions (BioRad, Hercules, Calif.).

Other biochemical assays

Esterase activity was determined by monitoring the hydrolysis of 100 nM fluorescein diacetate by HaCaT cell homogenates and their subcellular fractions, as reported elsewhere [32]. Fluorescence was monitored at an excitation wavelength of 400 nm and an emission wavelength of 530 nm, by means of a Perkin Elmer LS50B fluorometer (PerkinElmer Life and Analytical Sciences, Boston, Mass.). For cholesterol quantitation, membrane lipids were extracted from HaCaT subcellular fractions as described previously [33], and the content of cholesterol was measured by its conversion to cholestenone through cholesterol oxidase activity (kit from Boehringer Mannheim, Darmstadt, Germany), as previously reported [33, 34]. The level of CAV-1 in HaCaT subcellular fractions was quantified by enzyme-linked immunosorbent assay (ELISA), coating wells with homogenates (50 µg protein/well) as reported [22]. Anti-CAV-1 polyclonal antibodies (diluted 1:200) were used as first antibody, and goat anti-rabbit alkaline phosphatase conjugates (1:2000) as second antibody [22]. Color development of the alkaline phosphatase reaction was measured at 405 nm with p-nitrophenyl phosphate as substrate. Controls were carried out using non-immune rabbit serum, and included wells coated with different amounts of BSA [22]. The specificity of anti-CAV-1 antibodies was ascertained by Western blot analysis, showing that in HaCaT cell extracts they recognized a single immunoreactive band of the expected molecular size of CAV-1. These data (not shown) extend a previous report [35].

Preparation of membrane vesicles

A monodisperse solution of membrane vesicles of controlled average size was prepared without the addition of organic solvents or detergents, using the syringe-based plunger system Liposofast Extruder (Avestin, Ottawa, Canada) [36]. Briefly CM, PM and MM fractions, isolated from HaCaT cells (300×10^6) as described above, were first resuspended in PBS to give large, multilamellar vesicles. Uniformly sized, unilamellar vesicles (approximately 100 nm in diameter) were obtained by repeatedly passing these samples through a polycarbonate filter with 100-nm pores. The homogeneous vesicle suspensions (CMV, PMV and MMV, respectively) were stored at 4 °C under nitrogen and were used for biochemical assays within 2–3 days.

Analysis of anandamide uptake

The uptake of 400 nM [^{3}H]AEA by the AEA membrane transporter (AMT) of intact HaCaT cells (2×10^6/test), or of CM, PM and MM vesicles, was performed as described previously [18], incubating the samples for 10 min in the presence of 5% BSA. This amount of BSA has been shown to minimize the non-cellular uptake of AEA [18], and indeed it reduced the amount of [^{3}H]AEA bound to the wells without cells at 37 °C to less than 10% of that in the absence of BSA. In addition, to discriminate non-carrier-mediated from carrier-mediated transport of AEA through cell membranes, [^{3}H]AEA uptake was also measured at 4 °C, and this uptake was subtracted from that at 37 °C [16]. The effect of 10 µM VDM11 [29] or 5 µM OMDM-1 [31], selective AMT inhibitors, or of 10 nM URB597, or of 100 nM SR141716, on the uptake of 400 nM [^{3}H]AEA was determined by adding each substance directly to the incubation medium.

Statistical analysis

Data reported in this paper are the mean (± SD) of at least three independent determinations, each in duplicate. Statistical analysis was performed by the non-parametric Mann-Whitney U test, elaborating experimental data by means of the InStat 3 program (GraphPAD Software for Science, San Diego, Calif.).

Results

FAAH is localized intracellularly, and is associated with the endoplasmic reticulum

To characterize the subcellular localization of FAAH in HaCaT cells, we performed confocal microscopy analysis using anti-FAAH polyclonal antibodies. The specificity of these polyclonals has already been demonstrated by Western blot analysis, showing that they recognize a single immunoreactive band of the expected molecular size of FAAH in HaCaT cell homogenates [22]. The basal level of FAAH expression in proliferating (growing) cells was already significantly 6 h after TPA/Ca treatment, and achieved a maximum on day 5 (fig. 1). To identify differentiating keratinocytes, HaCaT cells were stained together with K1, a marker of the epidermal differentiation program [37]. Figure 1 shows that FAAH immunoreactivity increased in K1-positive cells, thus demonstrating that FAAH expression was differentiation dependent. The results, showing a time-dependent increase of FAAH protein, were superimposable on those recently reported for FAAH activity in the same cells [22], further demonstrating that TPA/Ca-induced differentiation is paralleled by increased FAAH expression. To rule out possible artifacts, antibody specificity was further ascertained by competition assays [22], performed by preincubating (at a 1:50 molar ratio) the anti-FAAH polyclonals with the immunogenic peptide used to elicit them (Primm, Milan, Italy). FAAH immunoreactivity was competed away by excess peptide antigen (fig. 2C), corroborating the specificity of the anti-FAAH antibodies used in the immunolocalization studies. Based on this evidence, and on the previous observation that AMT activity also increased time-dependently in HaCaT cells treated with TPA/Ca [22], we chose keratinocytes exposed to TPA/Ca for 24 h

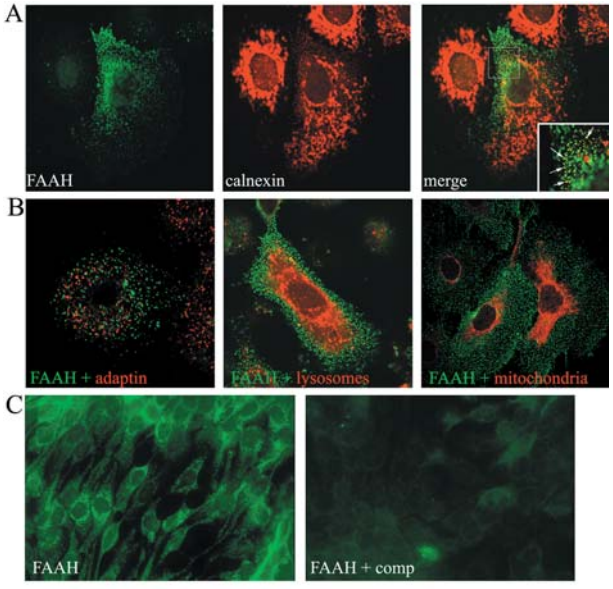

Figure 2. Cellular localization of FAAH in human keratinocytes. HaCaT cells were treated with TPA/Ca for 24 h, then stained with the indicated antibodies for confocal laser-scanning microscopy. Images are representative of at least three independent experiments, and five fields were examined for each treatment. (*A*) To assess potential co-localization of FAAH with endoplasmic reticulum, HaCaT cells were co-stained with anti-FAAH (in green) and anti-calnexin (in red) antibodies. Superimposition of the two stainings (merge) revealed a vesicular region of the endoplasmic reticulum where FAAH and calnexin perfectly overlapped (yellow). Dot structures, where FAAH and calnexin co-localized, are indicated by the white arrows in the inset at the bottom of the merge panel. The remaining part of the reticulum, with lamellar appearance, did not display any co-localization of the two proteins. (*B*) Double-staining with antibodies against FAAH and three other markers of subcellular compartments (adaptin, to stain clathrin-associated vesicles; LysoTracker Red DND-99, to stain lysosomes; and MitoTracker Red CMX Ros, to stain mitochondria) did not show any appreciable co-localization. (*C*) Specificity of the anti-FAAH antibody was tested by competition assay. Cells were stained with anti-FAAH antibody alone (FAAH), or after pre-incubation with an excess of peptide antigen (FAAH + comp).

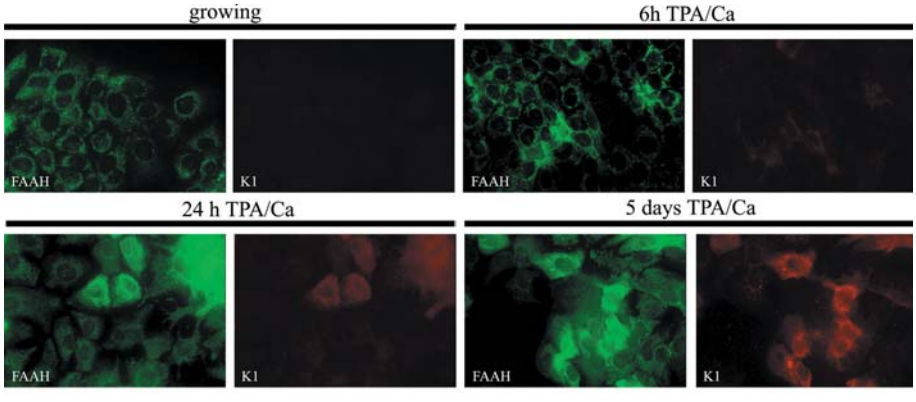

Figure 1. Expression of FAAH in differentiating human keratinocytes. HaCaT cells were kept in proliferating (growing) and differentiating (TPA/Ca) conditions for 6 h, 24 h and 5 days. Endogenous FAAH (in green) was detected by confocal microscopy using specific anti-FAAH antibody. The differentiation state of keratinocytes was assessed by co-staining HaCaT cells with anti-keratin1 (K1, in red) antibody. The expression of FAAH increased time-dependently in differentiating cells, as confirmed by comparing the immunoreactivity of FAAH in K1-positive and K1-negative cells. Images are representative of at least three independent experiments, and five fields were examined for each treatment.

to investigate further the spatial and functional relationship between AMT and FAAH.

To define the intracellular localization of FAAH in human keratinocytes, we performed a series of co-staining experiments with specific markers of subcellular compartments: calnexin was used to stain rough endoplasmic reticulum; adaptin to stain clathrin-coated vesicles; MitoTracker Red CMX Ros to stain mitochondria; and LysoTracker Red DND-99 to stain lysosomes. After 24 h of TPA/Ca stimulation, cells were fixed and examined by double staining immunofluorescence with the indicated antibodies. Anti-FAAH antibody revealed several dotted structures widely diffused in the cytoplasm, and sometimes particularly prominent in the perinuclear zone (fig. 2A, B). In agreement with other localization studies performed by subcellular fractionation [38–40], we did not observe any significant immunoreaction of FAAH inside the nucleus or on the plasma membrane. Furthermore, we observed that the distribution of these FAAH-positive vesicles was independent of the differentiation state of the cells (data not shown), suggesting that the intracellular localization of FAAH does not change during differentiation. The vesicular-like staining of FAAH appeared to overlap, even if partially, with that of calnexin (fig. 2A), but not with the other markers tested (fig. 2B). Finally, the immunofluorescence data demonstrated that a significant pool of FAAH specifically associates with a vesicular compartment of the endoplasmic reticulum, as already decribed in other cell lines [24].

FAAH activity resides in the endoplasmic compartment

The intracellular localization of FAAH was confirmed biochemically by measuring AEA hydrolysis in separated subcellular fractions. Briefly, HaCaT cells were lysed and crude membrane (CM) preparations were fractionated by equilibrium sedimentation in Percoll gradient, to obtain two different subfractions: intracellular microsomal membranes (MMs), and cell surface plasma membranes (PMs). Since our goal was to separate PMs from MMs, these two fractions were characterized by comparing the distribution of specific enzyme markers: alkaline phosphatase for PMs, and NADPH cytochrome *c* reductase for MMs. As summarized in table 1, the specific activity of NADPH cytochrome *c* reductase in MM fractions was approximately five-fold higher than that found in PM fractions, while the specific activity of alkaline phosphatase in the MM fraction was approximately-ten-fold lower than that in PM fractions. The activity of each enzyme marker in cell extracts was within the linearity range of the corresponding assay. On the basis of these results, we could conclude that, while PM preparations were primarly constituted of plasma membrane fragments, MM fractions consisted predominantly of membranes of intracellular origin.

Table 1. Characterization of HaCaT cell membrane subfractions. HaCaT cells were subfractionated as described in 'Materials and methods'. Alkaline phosphatase activity and NADPH cytochrome *c* reductase activity were expressed as percentage of the activity measured in the crude membrane fraction, set to 100. Values are given as the mean ± SD of three independent experiments. Values in parentheses represent percentage of plasma membranes, set to 100.

Subcellular fraction	Alkaline phosphatase (%)	NADPH-cytochrome *c* reductase (%)
Crude membranes	100 ± 10[a]	100 ± 11[b]
Plasma membranes	415 ± 20 (100%)	48 ± 5 (100%)
Microsomal membranes	54 ± 7 (13%)*	260 ± 10 (542%)*

* $p < 0.01$ versus plasma membranes.
[a] 100% = 37 ± 4 mU per milligram protein.
[b] 100% = 0.27 ± 0.03 mU per milligram protein.

We then measured FAAH activity in homogenates of whole HaCaT cells, and CM, PM, and MM fractions, in the presence or not of the FAAH inhibitors MAFP [29] and URB597 [30]. Consistent with the immunofluorescence data, FAAH activity associated with the microsomal compartment was about ten-fold higher than that of PM fractions, and was minimized by MAFP or URB597 (fig. 3A). Conversely, neither the AMT inhibitor OMDM-1 [31] nor the CB1 receptor antagonist SR141716 [18] affected FAAH activity in HaCaT cells or their subcellular fractions (fig. 3A). Interestingly, most (~80%) of FAAH specific activity (i.e., the activity normalized to the protein content) was retained by CM preparations compared with whole-cell extracts (fig. 3A). Additionally, the total activity of FAAH in a typical subfractionation experiment was ~4800, ~1680, ~20 and ~110 pmol/min in whole HaCaT cells, CM, PM, or MM fractions, respectively, demonstrating that total AEA hydrolysis was much higher in MMs than in PMs. Taken together, these findings demonstrate that FAAH is localized intracellularly, and mostly in calnexin-coated vesicles.

AEA accumulates in vesicles derived from plasma membranes, but not in those derived from intracellular membranes

To investigate the transport of AEA through cell membranes, we prepared intact unilamellar vesicles from purified membrane fractions, as described in 'Materials and methods'. Monodisperse solutions of unilamellar vesicles of CM, PM, and MM fractions, called CMV, PMV, and MMV, respectively, were used to assay AEA uptake. We found that vesicles of MM, rich in FAAH activity (fig. 3A), were virtually unable to take up AEA (fig. 3B), whereas vesicles of PM, essentially devoid of FAAH (fig. 3A), showed an AEA uptake about ten-fold higher than that of MMVs (fig. 3B). Uptake of AEA was

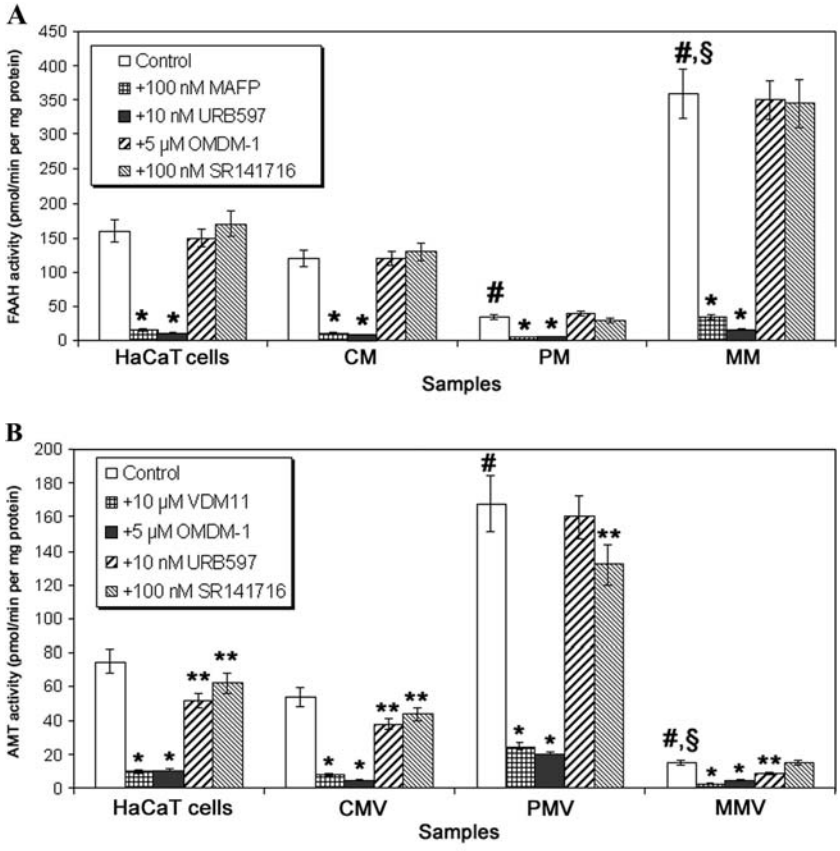

Figure 3. AEA degradation in subcellular fractions of human keratinocytes. HaCaT cell fractions were prepared and assayed as described in 'Materials and methods'. Values are given as mean ± SD of three independent experiments. In both panels, *$p < 0.01$ *versus* corresponding control; **$p < 0.05$ versus corresponding control; $^{\#}p < 0.01$ versus CM (or CMV); $^{\S}p < 0.01$ versus PM (or PMV). (*A*) AEA hydrolysis by FAAH activity was assayed in homogenates of whole HaCaT cells, and in their crude membranes (CM), plasma membranes (PM), or microsomal membranes (MM). The FAAH inhibitors MAFP and URB597, the AMT inhibitor OMDM-1 and the CB1 receptor antagonist SR141716 were added to each sample at the indicated concentrations. (*B*) AEA uptake through AMT activity was assayed in intact HaCaT cells, and in vesicles derived from their crude membranes (CMV), plasma membranes (PMV), or microsomal membranes (MMV). The AMT inhibitors VDM11 and OMDM-1, URB597 and SR141716 were added to each sample at the indicated concentrations.

always completely blocked by 10 μM VDM11 [29] or 5 μM OMDM-1 [31], selective AMT inhibitors. In addition, 10 nM URB597 caused a ~30% reduction of AMT activity in whole HaCaT cells, CMVs and MMVs, without affecting AEA uptake by PMVs (fig. 3B). A similar effect was observed upon incubation with 100 nM SR141716, which reduced by ~20% AMT in HaCaT cells, CMVs and PMVs, but not in MMVs (fig. 3B). Interestingly, most (~75%) AMT specific activity was retained by CMV preparations, compared with intact HaCaT cells (fig. 3B). Additionally, the total activity of AMT in a typical subfractionation experiment was ~2250, ~750, ~100, and ~5 pmol/min in whole HaCaT cells, CMVs, PMVs or MMVs, respectively, demonstrating that total AEA transport was much higher in PMs than in MMs. Taken together, these data favor the hypothesis that AEA enters the cells via an AMT-mediated mechanism rather than through a simple diffusion driven by FAAH, and that CB1 receptors can partially contribute to this process [18].

Further analysis of factors that may influence AEA transport

Specific anti-AMT antibodies are not yet available to visualize by confocal microscopy the putative AEA transporter. However, recently, a fluorescent substrate for AMT has been developed, SKM 4-45-1, which might prove useful for confocal studies [32]. With the perspective of using this compound, which is not yet commercially available, we assayed esterase activity in extracts of HaCaT cells and their subcellular fractions. In fact, SKM 4-45-1 must be hydrolyzed by esterase activity to become fluorescent [32]. We found that whole HaCaT cells had esterase activity of 220 ± 20 fluorescence units/min per milligram protein, whereas in crude membrane preparations this activity was much lower (~15%), and in plasma membrane or microsomal membrane fractions, it was not detectable at all. These findings are consistent with a cytosolic localization of esterase activity [32], and demonstrate that SKM-4-45-1 cannot be used to visualize AEA transport in vesicles reconstituted from membrane frac-

Table 2. Cholesterol content and CAV-1 expression in subcellular fractions of HaCaT cells.

Subcellular fraction	Cholesterol content (%)	CAV-1 expression (%)
Crude membranes	100 ± 11[a]	100 ± 9[b]
Plasma membranes	390 ± 50*	180 ± 20*
Microsomal membranes	18 ± 4*	N.D.

HaCaT cells were subfractionated as described in 'Materials and methods'. Membrane cholesterol content and CAV-1 expression were reported as percentage of the values of crude membranes, set to 100. Values are given as the mean ± SD of three independent experiments. N.D., not detectable; *$p < 0.01$ versus crude membranes.
[a] 100% = 97 ± 12 nmol per milligram protein.
[b] 100% = 0.220 ± 0.020 absorbance units at 405 nm per milligram protein.

tions devoid of cytosolic esterases. Along the same line, SKM 4-45-1 was recently used to co-localize AEA transport in caveolin-rich membranes of RBL-2H3 cells, leading to the suggestion that 'AEA uptake may occur via a caveolae/lipid raft-related endocytic process' [41]. Since lipid rafts are specialized plasma membrane microdomains that are enriched in cholesterol [41], and HaCaT cells express the caveolar marker protein CAV-1 [35], we checked our subcellular fractions for membrane cholesterol content and CAV-1 expression. We found that cholesterol and CAV-1 were present in the CM fractions and in higher amounts (about four-fold and two-fold, respectively) in PM fractions; instead, both compounds were present in very low or not detectable amounts in microsomal membranes (table 2). These findings are consistent with a much lower content of cholesterol in microsomal membranes compared with plasma membranes [42], where also CAV-1 is also localized [35, 41]. Incidentally, cholesterol levels found here in CM fractions of HaCaT cells were in keeping with those recently reported in synaptosomes from rat brain [34].

Discussion

The interruption of AEA signaling is thought to occur via a two-step process consisting of cellular uptake and intracellular hydrolysis by FAAH. A still unresolved, though critical, issue in endocannabinoid research is the mechanism by which AEA is transported inside the cells. Since the intracellular accumulation of AEA is known to be temperature dependent, saturable, substrate specific, and subjected to specific inhibition by arachidonic acid derivatives, a selective AEA membrane transport (AMT) has been postulated [15, 16]. However, the molecular identity of AMT remains unknown, and at present, molecular probes to test its expression at the protein or messenger RNA level are not available [14]. In addition, the kinetic features of AEA uptake do not rule out other mechanisms of transmembrane transport, being compatible, for example, with a simple diffusion driven by FAAH-catalyzed hydrolysis of AEA [23]. In this regard, whether and to what extent FAAH activity may control the uptake of AEA is still unclear. Interestingly, recent experimental efforts, using novel and more selective inhibitors of AEA uptake and/or FAAH knockout mice, have suggested that AEA transport is mediated by a combination of FAAH-dependent and FAAH-independent processes [18, 20, 21]. In addition, a recent paper, which appeared during the preparation of this manuscript, has provided evidence that in RBL-2H3 cells, AEA uptake occurs via a caveolae/lipid raft-related endocytic process, which is likely to occur through a protein-mediated mechanism [41].

In the present study, we sought to address the issue of the contribution of FAAH to AEA uptake by a direct approach, i.e., the physical separation of these two activities in cultured human keratinocytes. To this end, we examined by confocal microscopy the expression and cellular localization of FAAH in HaCaT cells, a non-tumorigenic line of immortalized keratinocytes, in which we have recently documented a fully functional 'endocannabinoid system' [22]. Then, we measured FAAH and AMT activity in different subcellular compartments, whereas the lack of specific anti-AMT antibodies mean that the confocal microscopy study could not be extended to the putative AEA transporter. We had previously observed that FAAH and AMT activity increase time-dependently upon TPA/Ca-induced differentiation of HaCaT cells [22]. These activity data were confirmed here by confocal microscopy of FAAH (fig. 1), pointing toward a potential role for this enzyme in skin physiology [3, 22]. Thus, we chose TPA/Ca-treated cells, expressing high AMT and FAAH activity [22], as a suitable model to attempt the spatial and functional separation of AEA hydrolysis and transport. FAAH immunoreactivity appeared to be localized intracellularly as a vesicular-like staining. This punctuate pattern, which increased but did not relocalize during cell differentiation, overlapped partially with that of calnexin, an endoplasmic reticulum marker. Unfortunately, we could not further define the subcellular distribution of FAAH, because a significant pool of this enzyme resides inside vesicular-like structures that could not be identified with the available tools. Previous immunocytochemical studies suggested that FAAH may be concentrated in other regions of the endomembane compartment, including mitochondria and the Golgi apparatus [24, 25]. Consistent with these reports and with the morphological data shown here, we found that FAAH enzymatic activity was associated with membranes of the endoplasmic reticulum, and excluded from the plasma membranes. Of note is that, whatever the fine distribution

of FAAH within the cell, on the basis of the reported data we can conclude that in human keratinocytes, FAAH is spatially excluded from the plasma membranes, i. e., from the site where AEA uptake takes place.

Next, to evaluate whether the spatial separation between AEA hydrolysis and AEA transport may also reflect a functional independence of the two processes, we reconstituted unilamellar vesicles from different membrane fractions, and assayed their AEA uptake activity. As expected, we found that AEA transport was associated with the plasma membrane vesicles, while it was essentially absent in microsome-derived vesicles. Thus, the distribution of AEA uptake was clearly distinct from that of AEA hydrolysis, mediated by FAAH almost exclusively in microsomal vesicles (compare fig. 3A, B). Overall, these results seem to rule out AEA uptake as the result of a simple diffusion driven by FAAH-mediated AEA hydrolysis. Instead, they seem to give further support to the presence of an AEA-specific transporter (AMT) on the plasma membrane of HaCaT cells. Keeping in mind that the kinetic properties of AMT and FAAH in these keratinocytes resemble those of many other cell types [1, 22, 43], one could suggest that the independence of AMT from FAAH shown here could have a broader validity. HaCaT cells express CB1 receptors on their surface [22], and these receptors have been recently reported to contribute to AEA uptake [18]. In keeping with previous data [18], AMT activity was partly inhibited (by ~20%) by the CB1 receptor antagonist SR141716 in intact HaCaT cells and in those vesicles containing plasma membranes, but not in microsomal vesicles (fig. 3B). Additionally, the FAAH inhibitor URB597 reduced AMT activity to a similar extent (by ~30%) in intact HaCaT cells and in vesicles reconstituted from crude membranes or microsomal membranes. However, it was ineffective on AMT in plasma membrane vesicles (fig. 3B), which are almost devoid of FAAH activity (fig. 3A). Taken together, these data confirm that FAAH and CB1 receptors can contribute to (but are not necessary for) AEA transport in HaCaT cells, as they do in neuronal cells [18]. A further point of interest is the association of AEA transport with caveolae/lipid rafts [41]. Here, we demonstrated that AMT activity is present in HaCaT cells and in those vesicles that contain cholesterol and CAV-1 (compare fig. 3B and table 2). In fact, vesicles reconstituted from PM fractions have an approximately three-fold increased AMT activity compared to CMVs, and they also contain higher amounts of cholesterol (about four-fold) and CAV-1 (about two-fold). Therefore, the activity of AMT and the content of cholesterol/CAV-1 seem to correlate linearly. Overall, these data seem to favor the 'endocytic hypothesis' proposed by McFarland et al. [41], and suggest that AEA uptake may benefit from a lipid environment enriched in cholesterol and CAV-1. Incidentally, a direct interaction of cholesterol with AEA, already reported for other N-acyl-hanolamines [44], might further contribute to enhance the transport process.

In conclusion, by means of confocal microscopy, subcellular fractionation, and biochemical analysis, we were able to 'uncouple' for the first time transport and hydrolysis of AEA in cells with a normal genetic background for FAAH, showing that they are two spatially and functionally independent events of the AEA inactivation pathway. These data may help to address the future development of therapeutic drugs for the treatment of an ever-increasing number of pathological conditions, as recently reviewed by Di Marzo et al. [45]. Incidentally, these findings open the question of how AEA is transported within the cell cytosol, implying the existence of an 'AEA intracellular transporter' (AIT), which should bring this lipid molecule to its final destination. In fact, as a caveat, such a soluble intracellular carrier might contribute significantly to AEA transport in whole cells, although it would be lost in the subfractionation experiments. However, the identity of both AMT and AIT await further analysis.

Acknowledgements. We wish to thank Prof. A. Finazzi Agrò (University of Rome 'Tor Vergata') for continuos interest and support to our work, and Prof. G. Melino (University of Rome 'Tor Vergata') for kind hospitality in his laboratory at the beginning of this project. We also thank Dr. M. Ranalli (University of Rome 'Tor Vergata') for his precious assistance with the confocal microscopy. Finally, we are grateful to Ministero dell'Istruzione, dell'Università e della Ricerca (COFIN 2003 to M. M., Rome), and to Fondazione Tercas (Convenzione 2004 to M. M., Teramo) for financial support.

1 Maccarrone M. and Finazzi-Agrò A. (2002) Endocannabinoids and their actions. Vitam. Horm. **65:** 225–255
2 Cravatt B. F., Prospero-Garcia O., Siuzdak G., Gilula N. B., Henriksen S. J., Boger D. L. et al. (1995) Chemical characterization of a family of brain lipids that induce sleep. Science **268:** 1506–1509
3 Calignano A., La Rana G., Giuffrida A. and Piomelli D. (1998) Control of pain initiation by endogenous cannabinoids. Nature **394:** 277–281
4 Lichtman A. H., Hawkins E. G., Griffin G. and Cravatt B. F. (2002) Pharmacological activity of fatty acid amides is regulated, but not mediated, by fatty acid amide hydrolase in vivo. J. Pharmacol. Exp. Ther. **302:** 73–79
5 Sugiura T., Kobayashi Y., Oka S. and Waku K. (2002) Biosynthesis and degradation of anandamide and 2-arachidonoylglycerol and their possible physiological significance. Prostaglandins Leukot. Essent. Fatty Acids **66:** 173–192
6 De Petrocellis L., Cascio M. G. and Di Marzo V. (2004) The endocannabinoid system: a general view and latest additions. Br. J. Pharmacol. **141:** 765–774
7 Devane W. A., Hanus L., Breuer A., Pertwee R. G., Stevenson L. A., Griffin G. et al. (1992) Isolation and structure of a brain constituent that binds to the cannabinoid receptor. Science **258:** 1946–1949
8 Fride E. and Mechoulam R. (1993) Pharmacological activity of the cannabinoid receptor agonist, anandamide, a brain constituent. Eur. J. Pharmacol. **231:** 313–314
9 Mechoulam R., Panikashvili D. and Shohami E. (2002) Cannabinoids and brain injury: therapeutic implications. Trends Mol. Med. **8:** 58–61

10 Cravatt B. F. and Lichtman A. H. (2003) Fatty acid amide hydrolase: an emerging therapeutic target in the endocannabinoid system. Curr. Opin. Chem. Biol. **7:** 469–475
11 Deutsch D. G., Ueda N. and Yamamoto S. (2002) The fatty acid amide hydrolase (FAAH). Prostaglandins Leukot. Essent. Fatty Acids **66:** 201–210
12 Bracey M. H., Hanson M. A., Masuda K. R., Stevens R. C. and Cravatt B. F. (2002) Structural adaptations in a membrane enzyme that terminates endocannabinoid signaling. Science **298:** 1793–1796
13 McKinney M. K. and Cravatt B. F. (2003) Evidence for distinct roles in catalysis for residues of the serine-serine-lysine catalytic triad of fatty acid amide hydrolase. J. Biol. Chem. **278:** 37393–37399
14 Hillard C. J. and Jarrahian A. (2003) Cellular accumulation of anandamide: consensus and controversy. Br. J. Pharmacol. **140:** 802–808
15 Beltramo M., Stella N., Calignano A., Lin S. Y., Makriyannis A. and Piomelli D. (1997) Functional role of high-affinity anandamide transport, as revealed by selective inhibition. Science **277:** 1094–1097
16 Hillard C. J., Edgemond W. S., Jarrahian A. and Campbell W. B. (1997) Accumulation of N-arachidonoylethanolamine (anandamide) into cerebellar granule cells occurs via facilitated diffusion. J. Neurochem. **69:** 631–638
17 Deutsch D. G., Glaser S. T., Howell J. M., Kunz J. S., Puffenbarger R. A., Hillard C. J. et al. (2001) The cellular uptake of anandamide is coupled to its breakdown by fatty-acid amide hydrolase. J. Biol. Chem. **276:** 6967–6973
18 Ortega-Gutierrez S., Hawkins E. G., Viso A., Lopez-Rodriguez M. L. and Cravatt B. F. (2004) Comparison of anandamide transport in FAAH wild-type and knockout neurons: evidence for contributions by both FAAH and the CB1 receptor to anandamide uptake. Biochemistry **43:** 8184–8190
19 Fowler C. J., Tiger G., Ligresti A., Lopez-Rodriguez M. L. and Di Marzo V. (2004) Selective inhibition of anandamide cellular uptake versus enzymatic hydrolysis – a difficult issue to handle. Eur. J. Pharmacol. **492:** 1–11
20 Fegley D., Kathuria S., Mercier R., Li C., Goutopoulos A., Makriyannis A. and Piomelli D. (2004) Anandamide transport is independent of fatty-acid amide hydrolase activity and is blocked by the hydrolysis-resistant inhibitor AM1172. Proc. Natl. Acad. Sci. USA **101:** 8756–8761
21 Ligresti A., Morera E., Van Der S. M., Monory K., Lutz B., Ortar G. et al. (2004) Further evidence for the existence of a specific process for the membrane transport of anandamide. Biochem. J. **380:** 265–272
22 Maccarrone M., Di Rienzo M., Battista N., Gasperi V., Guerrieri P., Rossi A. et al. (2003) The endocannabinoid system in human keratinocytes: evidence that anandamide inhibits epidermal differentiation through CB1 receptor-dependent inhibition of protein kinase C, activation protein-1, and transglutaminase. J. Biol. Chem. **278:** 33896–33903
23 Glaser S. T., Abumrad N. A., Fatade F., Kaczocha M., Studholme K. M. and Deutsch D. G. (2003) Evidence against the presence of an anandamide transporter. Proc. Natl. Acad. Sci. USA **100:** 4269–4274
24 Romero J., Hillard C. J., Calero M. and Rabano A. (2002) Fatty acid amide hydrolase localization in the human central nervous system: an immunohistochemical study. Brain Res. Mol. Brain Res. **100:** 85–93
25 Morozov Y. M., Ben Ari Y. and Freund T. F. (2004) The spatial and temporal pattern of fatty acid amide hydrolase expression in rat hippocampus during postnatal development. Eur. J. Neurosci. **20:** 459–466
26 Smart E. J., Ying Y. S., Mineo C. and Anderson R. G. (1995) A detergent-free method for purifying caveolae membrane from tissue culture cells. Proc. Natl. Acad. Sci. USA **92:** 10104–10108
27 Engstrom L. (1961) Studies on calf-intestinal alkaline phosphatase. I. Chromatographic purification, microheterogeneity and some other properties of the purified enzyme. Biochim. Biophys. Acta **52:** 36–48
28 Williams C. H. Jr and Kamin H. (1962) Microsomal triphosphopyridine nucleotide-cytochrome c reductase of liver. J. Biol. Chem. **237:** 587–595
29 De Petrocellis L., Bisogno T., Maccarrone M., Davis J. B., Finazzi-Agro A. and Di Marzo V. (2001) The activity of anandamide at vanilloid VR1 receptors requires facilitated transport across the cell membrane and is limited by intracellular metabolism. J. Biol. Chem. **276:** 12856–12863
30 Kathuria S., Gaetani S., Fegley D., Valino F., Duranti A., Tontini A. et al. (2003) Modulation of anxiety through blockade of anandamide hydrolysis. Nat. Med. **9:** 76–81
31 Ortar G., Ligresti A., De Petrocellis L., Morera E. and Di Marzo V. (2003) Novel selective and metabolically stable inhibitors of anandamide cellular uptake. Biochem. Pharmacol. **65:** 1473–1481
32 Muthian S., Nithipatikom K., Campbell W. B. and Hillard C. J. (2000) Synthesis and characterization of a fluorescent substrate for the N-arachidonoylethanolamine (anandamide) transmembrane carrier. J. Pharmacol. Exp. Ther. **293:** 289–295
33 Maccarrone M., Navarra M., Catani V., Corasaniti M. T., Bagetta G. and Finazzi-Agrò A. (2002) Cholesterol-dependent modulation of the toxicity of HIV-1 coat protein gp120 in human neuroblastoma cells. J. Neurochem. **82:** 1444–1452
34 Mitter D., Reisinger C., Hinz B., Hollmann S., Yelamanchili S. V., Treiber-Held S. et al. (2003) The synaptophysin/synaptobrevin interaction critically depends on the cholesterol content. J. Neurochem. **84:** 35–42
35 Czarny M., Lavie Y., Fiucci G. and Liscovitch M. (1999) Localization of phospholipase D in detergent-insoluble, caveolin-rich membrane domains: modulation by caveolin-1 expression and caveolin-182-101. J. Biol. Chem. **274:** 2717–2724
36 Walde P. and Ichikawa S. (2001) Enzymes inside lipid vesicles: preparation, reactivity and applications. Biomol. Eng. **18:** 143–177
37 Boukamp P., Petrussevska R. T., Breitkreutz D., Hornung J., Markham A. and Fusenig N. E. (1988) Normal keratinization in a spontaneously immortalized aneuploid human keratinocyte cell line. J. Cell Biol. **106:** 761–771
38 Schmid P. C., Zuzarte-Augustin M. L. and Schmid H. H. (1985) Properties of rat liver N-acylethanolamine amidohydrolase. J. Biol. Chem. **260:** 14145–14149
39 Hillard C. J., Wilkison D. M., Edgemond W. S. and Campbell W. B. (1995) Characterization of the kinetics and distribution of N-arachidonylethanolamine (anandamide) hydrolysis by rat brain. Biochim. Biophys. Acta **1257:** 249–256
40 Maurelli S., Bisogno T., De Petrocellis L., Di Luccia A., Marino G. and Di Marzo V. (1995) Two novel classes of neuroactive fatty acid amides are substrates for mouse neuroblastoma "anandamide amidohydrolase". FEBS Lett. **377:** 82–86
41 McFarland M. J., Porter A. C., Rakhshan F. R., Rawat D. S., Gibbs R. A. and Barker E. L. (2004) A role for caveolae/lipid rafts in the uptake and recycling of the endogenous cannabinoid anandamide. J. Biol. Chem. **279:** 41991–41997
42 Liscum L. and Underwood K. W. (1995) Intracellular cholesterol transport and compartmentation. J. Biol. Chem. **270:** 15443–15446
43 Maccarrone M., Van Der S. M., Veldink G. A. and Finazzi-Agrò A. (2002) Inhibitors of endocannabinoid degradation as potential therapeutic agents. Curr. Med. Chem. Anti-Inflamm. Anti-Allergy Agents **1:** 103–113
44 Ramakrishnan M., Kenoth R., Kamlekar R. K., Chandra M. S., Radhakrishnan T. P. and Swamy M. J. (2002) N-Myristoylethanolamine-cholesterol (1:1) complex: first evidence

from differential scanning calorimetry, fast-atom-bombardment mass spectrometry and computational modelling. FEBS Lett. **531:** 343–347

45 Di Marzo V., Bifulco M. and De Petrocellis L. (2004) The endocannabinoid system and its therapeutic exploitation. Nat. Rev. Drug Discov. **3:** 771–784